American Mineralogist, Volume 87, pages 1342–1350, 2002

Experimental determination of the equilibria: rutile + magnesite = geikielite + CO_2 and zircon + 2 magnesite = baddeleyite + forsterite + 2 CO_2

JOHN M. FERRY,[1,2,*] ROBERT C. NEWTON,[2] AND CRAIG E. MANNING[2]

[1]Department of Earth and Planetary Sciences, Johns Hopkins University, Baltimore, Maryland 21218, U.S.A.
[2]Department of Earth and Space Sciences, University of California at Los Angeles, Los Angeles, California 90095, U.S.A.

ABSTRACT

The *P-T* conditions of both equilibria were determined precisely by reversal experiments in a piston-cylinder apparatus. On the basis of 8 experiments, brackets for the rutile-magnesite-geikielite equilibrium are 7.0–7.1 kbar at 800 °C, 8.6–8.7 kbar at 850 °C, and 10.5–10.7 kbar at 900 °C. On the basis of 9 experiments, brackets for the zircon-magnesite-baddeleyite-forsterite equilibrium are 7.1–7.7 kbar at 800 °C, 9.2–9.4 kbar at 850 °C, and 10.7–10.9 kbar at 900 °C. Considering experimental uncertainties in *P* (±300 bars) and *T* (±3 °C), equilibrium curves calculated from both the Berman and the Holland and Powell databases pass through all brackets. Molar Gibbs free energy of formation from the elements at 1 bar and 298 K for geikielite and zircon, derived from the experiments and consistent with the Berman database, are –1481.94 ± 0.67 kJ and –1917.54 ± 1.25 kJ, respectively. Corresponding values consistent with the Holland and Powell database are –1479.30 ± 0.74 kJ and –1918.47 ± 1.49 kJ. Application of the two equilibria indicate that: (1) the mole fraction of CO_2 in fluid was 0.54–1.00 when geikielite and baddeleyite formed during contact metamorphism of siliceous dolomites in the Ballachulish aureole, Scotland; (2) the activity of CO_2 could have been as low as $2 \cdot 10^{-5}$ during ultra-high pressure metamorphism of magnesite-bearing ecologites; and (3) the activity of CO_2 was <0.18 during one instance of mantle metasomatism.

INTRODUCTION

Geikielite (Gk) and baddeleyite (Bd) are common trace minerals in contact metamorphosed siliceous dolomitic limestones that develop during prograde metamorphism at the expense of detrital rutile (Rt) and zircon (Zrn) by the reactions:

$$\underset{\text{rutile}}{TiO_2} + \underset{\text{dolomite}}{CaMg(CO_3)_2} = \underset{\text{geikielite}}{MgTiO_3} + \underset{\text{calcite}}{CaCO_3} + \underset{\text{fluid}}{CO_2} \quad (1)$$

and

$$\underset{\text{zircon}}{ZrSiO_4} + 2\,\underset{\text{dolomite}}{CaMg(CO_3)_2} = \underset{\text{baddeleyite}}{ZrO_2} + \underset{\text{forsterite}}{Mg_2SiO_4} + 2\,\underset{\text{calcite}}{CaCO_3} + 2\,\underset{\text{fluid}}{CO_2} \quad (2)$$

[these and all other abbreviations for minerals follow Kretz (1983)]. Isograds can be mapped in contact aureoles based on reactions 1 and 2, and they lie at grades above that of the forsterite (Fo) isograd but below that of the periclase (Per) isograd (e.g., Ferry 1996a) where the major minerals in marbles are dolomite (Dol), calcite (Cal), and Fo. Equilibria involving Gk and Bd based on reactions 1 and 2 therefore offer the potential to constrain pressure (*P*) and the activity of CO_2 (a_{CO_2}) over a range of metamorphic conditions at which the major minerals in siliceous dolomitic marbles are uninformative. Furthermore, because Bd can be dated radiometrically, equilibria among Bd, Zrn, Dol, Cal, and Fo in principle can help define quantitatively the *P*-a_{CO_2}-tempertaure (*T*)-age conditions of a specific mineral reaction during metamorphism. In order for the potential to be realized fully, however, accurate thermodynamic data are required for Gk and Zrn, and this was the motivation for the phase equilibrium experiments. The reactions:

$$\underset{\text{rutile}}{TiO_2} + \underset{\text{magnesite}}{MgCO_3} = \underset{\text{geikielite}}{MgTiO_3} + \underset{\text{fluid}}{CO_2} \quad (3)$$

and

$$\underset{\text{zircon}}{ZrSiO_4} + 2\,\underset{\text{magnesite}}{MgCO_3} = \underset{\text{baddeleyite}}{ZrO_2} + \underset{\text{forsterite}}{Mg_2SiO_4} + 2\,\underset{\text{fluid}}{CO_2} \quad (4)$$

were investigated rather than reactions 1 and 2 because thermodynamic analysis of equilibria based on reactions 3 and 4 is uncomplicated by the effects of solid solution between Cal and Dol. Current thermodynamic databases (Berman 1988, updated 1992; Holland and Powell 1998, updated 2001) predict that reactions 1 and 3 and reactions 2 and 4 are almost parallel in *T*-*P* space separated by only 40–60 °C at constant *P*. Reactions 3 and 4 therefore are good analogs to reactions 1 and 2 and, furthermore, have direct application to coesite- and diamond-bear-

* E-mail: jferry@jhu.edu

ing ultrahigh-pressure (UHP) metamorphic rocks that contain magnesite (Mgs), Rt, and Zrn (Liou et al. 1995; Zhang and Liou 1996; Dobrzhinetskaya et al. 2001) and to diamond-bearing mantle samples that contain Zrn and Bd or Rt and Mg-rich ilmenite (Schärer et al. 1997; Zhao et al. 1999; Sobolev and Yefimova 2000).

EXPERIMENTAL METHODS

Apparatus

Experiments were conducted in a 2.54 cm-diameter, end-loaded, piston-cylinder apparatus using NaCl as the pressure medium and a cylindrical graphite heater sleeve [described in greater detail by Manning and Boettcher (1994)]. Pressure was raised at room T to 1–3 kbar below the target P, and T was then raised to the target T. Pressure was bled continuously between ≈600 °C and the target T to maintain the desired value of the experiment. Pressure was measured by a Heise gauge and maintained to within ±100 bars of the P_{ex} values reported in Tables 1 and 2. Temperature was measured and controlled with a Pt-$Pt_{90}Rh_{10}$ thermocouple that was separated from the sample capsule by a Pt shim ≈0.1 mm thick. Temperature was typically maintained within ±1 °C of the values reported in Tables 1 and 2 and in all cases within ±2 °C. Accuracy of the thermocouples at room P is ±1 °C or better. The standard convention is to apply no P correction to the thermocouple readings (e.g., Manning and Boettcher 1994). The uncertainty in the values of T reported in Tables 1 and 2 is therefore taken as ±3 °C.

Although the piston-cylinder apparatus is considered virtually frictionless under the conditions of the experiments (e.g., Manning and Boettcher 1994; Newton and Manning 2000), the assumption (as well as the calibration of the Heise gauge) was tested by a set of experiments on the equilibrium among brucite (Brc), Per, and H_2O fluid. Coarse cleavage fragments of Per [synthetized by Muscle Shoals Electrochemical Company and the same material used by Koziol and Newton (1995) and by Aranovich and Newton (1998)] were welded with distilled and deionized H_2O in 17-mm long, 5-mm diameter Pt capsules that were then folded into the same geometry as those used in the other phase-equilibrium experiments. An experiment that was brought to 851 °C and 11.0 kbar and then immediately quenched yielded approximately equal amounts of Per and Brc (estimated visually from a grain mount in immersion oil) because target P-T conditions were reached through the Brc stability field. Two other experiments at 851 °C of 5 h duration produced >95% Per at 10.8 kbar and >95% Brc at 11.2 kbar. The experiments reversed the Brc-Per-H_2O equilibrium at 851 °C between 10.8 and 11.2 kbar. The true P of the Brc-Per-H_2O equilibrium at 851 °C was considered that computed from the Holland and Powell (1998, updated 2001) database, 11.0 kbar. [For comparison, P of the Brc-Per-H_2O equilibrium at 851 °C predicted from the data of Berman (1988, updated 1992) is 11.1 kbar.] The P correction for the apparatus therefore was taken as 0±200 bars. Considering the ±100 bar variation in P during reversal experiments on reactions 3 and 4, values of P reported in Tables 1 and 2 are believed uncertain by no more than ±300 bars.

Starting materials

Starting materials used in the phase equilibrium experiments were synthetic minerals from a variety of sources. Magnesite was the same material used by Koziol and Newton (1995) synthesized in a Morey vessel from hydrous magnesium carbonate. Forsterite was the same material used by Charlu et al. (1975) synthesized from a melt by Union Carbide Co. X-ray diffraction (XRD) traces of both materials displayed peaks for Mgs and Fo only. Rutile, Gk, Zrn, and Bd were synthesized hydrothermally from laboratory reagents in the presence of distilled and deionized H_2O. Rutile was crystallized from TiO_2 at 787 °C and 10.0 kbar for 6 h. An XRD trace of the experimental product displayed only Rt peaks. A mixture of Gk and Rt was

TABLE 1. Reversed experimental data for the reaction: Rt + Mgs = Gk + CO_2 (reaction 3)

Experiment number	U17	U19	U10	U18	U11	U9	U13	U14
T(°C)	800°	800°	850°	850°	850°	850°	900°	900°
P_{ex} (kbar)*	7.3	7.6	8.9	9.0	9.2	9.3	10.9	11.3
Mix (mg)†	2.903	3.765	3.056	4.036	3.667	3.697	3.855	3.705
$Ag_2C_2O_4$ (mg)‡	2.129	2.409	1.835	2.661	2.252	2.198	2.023	2.017
Initial CO_2 (µg)§	589	667	508	736	623	608	560	558
t(h)#	28	25	25	26	25	25	10	11
ΔCO_2 (µg)‖	+142	–397	+486	–309	–33	–194	+97	–160
Stable assemblage**	Gk	Rt+Mgs	Gk	Rt+Mgs	Rt+Mgs	Rt+Mgs	Gk	Rt+Mgs
% reaction††	+32%	–68%	+100%	–50%	–6%	–34%	+16%	–28%
H_2O (µg)‡‡	14	14	17	6	20	16	17	15
X_{CO_2}§§	0.933	0.844	0.936	0.967	0.879	0.874	0.910	0.878
P_{cor} (kbar)##	7.1	7.0	8.6	8.8	8.7	8.7	10.5	10.7

* P of the experiment.
† Initial mass of mineral reactants and products.
‡ Initial mass of $Ag_2C_2O_4$.
§ Initial mass CO_2 after decomposition of $Ag_2C_2O_4$ (using measured mass yield of 95.5% of stoichiometric value).
# Duration of experiment.
‖ Weight loss at room T from punctured inner capsule after experiment minus initial mass CO_2 (positive values indicate progress of the decarbonation reaction, negative values indicate progress of the carbonation reaction).
** Inferred stable reactant or product minerals at conditions of experiment.
†† % reaction (positive for decarbonation, negative for carbonation).
‡‡ Weight loss of punctured inner capsule after baking at 300 °C for 10–20 min (assumed H_2O).
§§ X_{CO_2} of fluid at end of experiment computed from measured weight loss of punctured capsule at room T, after baking at 300 °C, and inferred CO-content (see text).
P corrected from P_{ex} and computed X_{CO_2} at end of experiment to value for equilibrium with pure CO_2 fluid (see text).

crystallized from a combination of MgO and TiO_2 with bulk composition MgO:TiO_2 = 1.0:1.1 (molar) at 850 °C and 15.0 kbar for 7 h. An XRD trace of the material displayed only Gk and Rt peaks. A combination of SiO_2 and ZrO_2 with bulk composition SiO_2:ZrO_2 = 1.0:1.1 (molar), crystallized at 850 °C and 15.0 kbar for 29 h, produced a mixture of Zrn and Bd with a few percents of quartz (as judged from an XRD trace). Sufficient ZrO_2 was added to change the bulk composition of the Zrn-Bd-quartz mixture to SiO_2:ZrO_2 = 1.0:2.0 (molar), and the new mixture was recrystallized at 850 °C and 15.0 kbar for 25 h. The product was a mixture of Zrn and Bd in the molar ratio 1:1 whose XRD trace displayed only Zrn and Bd peaks. Mineral starting material for experiments on reaction 3 was a combination of Rt, Mgs, and the Gk-Rt mixture to give minerals in the molar proportions Rt:Mgs:Gk = 1:1:1. Mineral starting material for experiments on reaction 4 was a combination of Fo, Mgs, and the Zrn-Bd mixture to give minerals in the molar proportions Zrn:Mgs:Bd:Fo = 1:2:1:1. The mineral starting mixtures were dispersed in an ethanol suspension onto a polished carbon or glass substrate, carbon coated, and examined with scanning back-scattered electron microscopy (SEM) using the JEOL JXA-8600 electron microprobe at Johns Hopkins University. Only the phases Rt, Mgs, Gk, Zrn, Bd, and Fo were observed. The source for CO_2 in the starting materials was commercial silver oxalate reagent (nominally $Ag_2C_2O_4$) which decomposes to Ag and CO_2 at the conditions of the experiments.

Experimental procedure

The design of the phase-equilibrium experiments followed that of Koziol and Newton (1995, 1998). Between 2.9 and 4.5 mg of the stoichiometric mineral mixtures were carefully weighed with a Metler M3 microbalance ($1\sigma = 2$ μg) and loaded into 13 mm long, 2 mm diameter Pt capsules with sufficient silver oxalate (1.8–4.9 mg) to produce CO_2 in excess of what could completely carbonate the mineral mixture. The capsules were arc-welded and folded in half. To minimize reduction of the CO_2 by H_2 evolved from the sample assembly (Rosenbaum and Slagel 1995), each sealed and folded capsule was placed in an outer 19 mm-long, 5 mm-diameter Pt capsule with 51.3–78.7 mg hematite (Hem) and 10.6–18.3 mg distilled and deionized H_2O. Loaded outer capsules were also arc-welded and folded in half. The double capsule was held at elevated *P* and *T* for 7–28 h.

Experiments were terminated by shutting off power to the apparatus. Within 20 s, *T* dropped to <200 °C and *P* dropped by ≈3 kbar. After the sample reached room *T*, the residual *P* was released over several min. The double capsule was washed in distilled and deionized H_2O and dried for 5 min at 115 °C in a 1-atm oven. With the exception of three experiments in Tables 1 and 2, all outer capsules exuded H_2O when punctured and contained abundant magnetite (Mag, produced during the experiment) and some unreacted Hem, confirming that oxygen and hydrogen fugacities were buffered at all times by Hem + Mag + H_2O. In two of the exceptions (U14, U40) Hem + Mag were present but not H_2O, and in the third (U36), Mag was present but neither Hem nor H_2O. Even in the case of these three exceptions, oxygen and hydrogen fugacities evidently were buffered by Hem + Mag + H_2O at the beginning of the experiment, which (as will be discussed further below) is sufficient to prevent significant reduction of CO_2 in the inner capsule. The inner capsule was removed, washed in distilled and deionized H_2O, dried for 5 min at 115 °C, and weighed. The inner capsule was then punctured with a steel needle (causing an audible hiss of released gas), weighed a second time, dried at 115 °C for 10–20 min, reweighed, dried at 300 °C in a 1-atm furnace for 10–20 min, and weighed again. The weight change between the first and second weighing was interpreted as loss of CO_2. In every case the weight change of the punctured inner capsule after drying at 115 °C was 0±2 μg. In all but one experiment (U29), however, there was a significant weight loss

TABLE 2. Reversed experimental data for the reaction: Zrn + 2 Mgs = Bd + Fo + 2 CO_2 (reaction 4)

Experiment number	U39	U29	U21	U40	U22	U23	U36	U30	U28
T (°C)	800°	800°	800°	850°	850°	850°	850°	900°	899°
P_{ex} (kbar)*	7.2	7.5	7.8	8.8	9.3	9.7	10.2	10.9	11.2
Mix (mg)†	3.522	3.871	4.174	3.178	4.289	4.195	4.472	4.469	3.914
$Ag_2C_2O_4$ (mg)‡	2.101	3.551	2.523	2.099	3.008	3.425	3.845	4.875	3.560
Initial CO_2 (μg)§	581	983	698	581	832	948	1064	1349	985
t (h)#	24	25	27	24	25	25	24	12	7
ΔCO_2 (μg)‖	+99	–8	–35	+469	+94	–133	–222	+33	–106
Stable assemblage**	Bd+Fo	NR	Zrn+Mgs	Bd+Fo	Bd+Fo	Zrn+Mgs	Zrn+Mgs	Bd+Fo	Zrn+Mgs
% reaction††	+20%	NR	–6%	+100%	+15%	–22%	–35%	+5%	–19%
H_2O (μg)‡‡	9	2	8	13	12	16	21	16	13
X_{CO_2}§§	0.962	0.995	0.971	0.955	0.961	0.934	0.914	0.963	0.955
P_{cor} (kbar)##	7.1	7.5	7.7	8.6	9.2	9.4	9.8	10.7	10.9

* *P* of the experiment.
† Initial mass of mineral reactants and products.
‡ Initial mass of $Ag_2C_2O_4$.
§ Initial mass CO_2 after decomposition of $Ag_2C_2O_4$ (using measured mass yield of 95.5% of stoichiometric value).
# Duration of experiment.
‖ Weight loss at room *T* from punctured inner capsule after experiment minus initial mass CO_2 (positive values indicate progress of the decarbonation reaction, negative values indicate progress of the carbonation reaction).
** Inferred stable reactant or product minerals at conditions of experiment. NR = no reaction within uncertainty of measurement.
†† % reaction (positive for decarbonation, negative for carbonation). NR = no reaction within uncertainty of measurement.
‡‡ Weight loss of punctured inner capsule after baking at 300 °C for 10–20 min (assumed H_2O).
§§ X_{CO_2} of fluid at end of experiment computed from measured weight loss of punctured capsule at room *T*, after baking at 300 °C, and inferred CO-content (see text).
P corrected from P_{ex} and computed X_{CO_2} at end of experiment to value for equilibrium with pure CO_2 fluid (see text).

of the punctured inner capsule after drying at 300 °C, 6–21 μg, which was interpreted as loss of H_2O.

Interpretation of weight measurements

CO_2 and H_2O contents of starting materials. Quantitative interpretation of the measured CO_2 and H_2O losses required accurate assessment both of the CO_2 content of the silver oxalate and of the amount of any H_2O adsorbed by the silver oxalate and the mineral starting materials. A CO_2 yield less than stoichiometric values was expected because silver oxalate gradually decomposes by photolysis. In three sets of measurements, 3.7–4.1 mg of silver oxalate were loaded into 13 mm-long, 5 mm-diameter Pt tubes and sealed by arc welding. The sealed Pt tubes were held at 300–400 °C for 10–60 min in a 1-atm furnace, weighed with the microbalance, punctured with a steel needle, and reweighed. The weight loss was interpreted as CO_2 evolved by the decomposition of silver oxalate and corresponded to yields 95.1, 95.5, and 95.7 wt% of the value expected from ideal stoichiometry. An average CO_2 yield of 95.5% stoichiometric was adopted for the silver oxalate. The punctured capsules were reheated at 300 °C for 10–60 min and weighed a third time. A small further decrease in weight, 2–4 μg, was interpreted as loss of adsorbed H_2O. The average adsorbed H_2O was 0.76 μg/mg silver oxalate. The amount of H_2O adsorbed onto the mineral starting materials was measured by loading 3.5 mg of the Rt-Mgs-Gk mix and 4.7 mg of the Zrn-Mgs-Bd-Fo mix into 13 mm-long, 2 mm-diameter Pt tubes that were sealed by arc welding. The sealed Pt tubes were held at 300 °C for 15–20 min in a 1-atm furnace, weighed with the microbalance, punctured with a steel needle, reheated to 300 °C for 15–20 min, and reweighed. The weight loss from the punctured capsules, 6–7 μg, was interpreted as loss of adsorbed H_2O. The Rt-Mgs-Gk mix adsorbed 1.73 μg H_2O/mg, and the Zrn-Mgs-Bd-Fo mix adsorbed 1.49 μg H_2O/mg. A similar measurement demonstrated that the synthetic Rt adsorbed no detectable H_2O. The Rt therefore was used in a final experiment to demonstrate that the CO_2 yield from silver oxalate at 1 atm was the same as the yield at *P-T* conditions of the phase-equilibrium experiments. A double capsule was prepared identical to those used in the phase-equilibrium experiments but with the mineral reaction mix replaced in the inner capsule by 7.3 mg synthetic Rt. The double capsule was held in the piston-cylinder apparatus at 850 °C and 9.0 kbar for 2 h, quenched, and analyzed in the usual fashion. The CO_2 loss from the inner capsule was 95.5% of the stoichiometric value for silver oxalate (the same within error of measurement as the 1-atm yields), and the loss of H_2O was 18 μg.

Analysis of experimental products. The stable mineral assemblage at the conclusion of the phase-equilibrium experiments was determined by subtracting the amount of CO_2 initially produced by the (calibrated) decomposition of silver oxalate from the CO_2 loss at the end of the experiment. If the difference, ΔCO_2 (Tables 1 and 2), was positive, a decarbonation reaction occurred during the experiment, and minerals corresponding to the decarbonated side of reaction 3 or 4 were stable. If ΔCO_2 was negative, a carbonation reaction occurred during the experiment, and minerals corresponding to the carbonated side of reaction 3 or 4 were stable. Measured absolute values of $\Delta CO_2 > 30$ μg were considered significant. One value of $\Delta CO_2 = -8$ μg (U29, Table 2), although barely outside weighing errors, was interpreted conservatively as a case of no reaction. Considering the measured mass of the mineral reaction mixtures in each experiment, measured values of ΔCO_2 were converted to a percentage reaction with the convention of (+) for decarbonation and (–) for carbonation (Tables 1 and 2).

The experimental products were gently disaggregated with an agate mortar and pestle, dispersed in an ethanol suspension onto a polished carbon or glass substrate, carbon coated, and examined with back-scattered SEM. The largest grains of each mineral were up to several μm in diameter and could be identified by qualitative energy-dispersive X-ray spectrometry. The direction of reaction determined from the weight-loss measurements was confirmed unequivocally in all experiments in which there was ≥20% reaction by qualitatively comparing the relative proportions of minerals in the experimental products with the stoichiometric proportions of minerals in the starting mixtures in SEM images. In all samples with ≥20% reaction, visual estimates of modes were correlated qualitatively with extent of reaction determined by weight loss. The direction of reaction in experiments in which there was <20% reaction could not be determined confidently by qualitative SEM observations of the experimental products.

Hydrogen diffusion. The H_2O loss from experimental charges at the end of most experiments was larger than can be explained by release of H_2O adsorbed on the silver oxalate and mineral starting materials. The additional H_2O most likely was produced by diffusion of H_2 from the sample assembly into the inner capsule where it reacted with CO_2 to form H_2O and CO by the reaction:

$$H_2 + CO_2 = CO + H_2O \quad (5)$$

(Rosenbaum and Slagel 1995). Measurable mass transport of H_2 occurred in spite of the presence of the Hem-Mag-H_2O buffer in the outer capsule separating the inner capsule from the rest of the sample assembly. The experiment involving synthetic Rt in place of a mineral reaction mix both unequivocally confirms H_2 diffusion into the inner capsules of the phase-equilibrium experiments and constrains the duration over which the process occurred. The Rt had no adsorbed H_2O and the silver oxalate (1.824 mg loaded) just 1 μg. No reaction was possible between Rt and either silver oxalate or its decomposition products at the *P-T* conditions of the experiment. Loss of H_2O from the inner capsule at the end of the 2 h experiment, however, was 18 μg. The only plausible explanation for the 18 μg H_2O loss is addition of H_2 to the inner capsule. Because the measured H_2O loss of 18 μg is within the range of H_2O losses in phase-equilibrium experiments lasting 24–28 h (Tables 1-2), H_2 transport must have been essentially complete within the first two hours of the phase-equilibrium experiments. The short duration of H_2 diffusion could be explained if the H_2 was produced by rapid dehydration of the nominally dry NaCl pressure medium and subsequent reaction of evolved H_2O with the hot graphite furnace.

Correction for H_2O in experimental charges. Because of H_2O adsorbed onto starting materials and produced by H_2 dif-

fusion at the start of the experiments, the phase-equilibrium experiments were not conducted in the presence of a pure CO_2 fluid. Judging from the calibrated CO_2 yield of the silver oxalate and the H_2O loss measured at the end of the experiments, the initial fluid composition in the inner capsule was usually $X_{CO_2} = 0.90–0.95$. For experiments conducted at P above the P-X_{CO_2} curve for reaction 3 or 4, a carbonation reaction occurred and fluid composition was driven to lower values of X_{CO_2} at the end of the experiment (Fig. 1). For experiments conducted at P below the relevant P-X_{CO_2} curve, a decarbonation reaction occurred and fluid composition was driven to larger values of X_{CO_2} at the end of the experiment. If equilibrium was attained, the X_{CO_2} at the end of the experiment and the P-X_{CO_2} curve at T of the experiment can be used to define the difference in P between that of the experiment (P_{ex}, Tables 1 and 2) and P of the equilibrium in the presence of pure CO_2 fluid (Fig. 1). Subtraction of the P correction from P_{ex} provides an estimate of the P for equilibrium of mineral reactants and products with pure CO_2 fluid (P_{cor}, Tables 1 and 2).

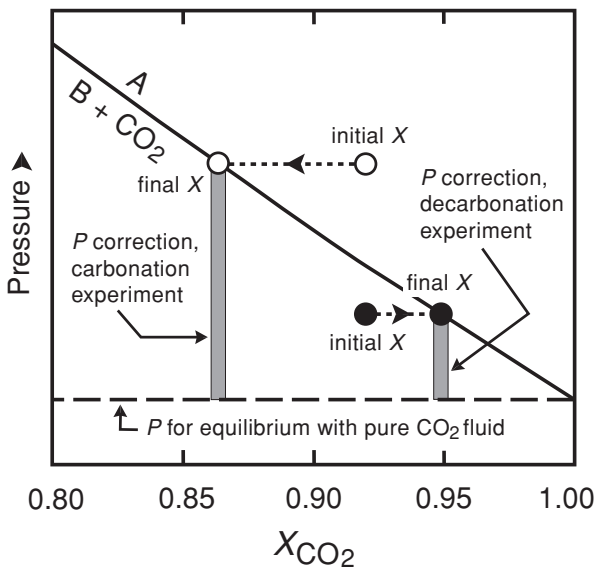

FIGURE 1. Schematic isothermal P-X_{CO_2} diagram for generic carbonation/decarbonation equilibrium A = B + CO_2 illustrating the P correction from that of the experiment to that for equilibrium between minerals and a pure CO_2 fluid. Because of H_2O adsorbed onto starting materials and produced by H_2 diffusion into the inner capsule, fluid at the beginning of the experiments typically had $X_{CO_2} = 0.90–0.95$ ("initial X"). Experiments at P above the equilibrium curve (open circles) resulted in progress of the carbonation reaction and a final X_{CO_2} ("final X") less than initial. Experiments at P below the equilibrium curve (filled circles) resulted in progress of the decarbonation reaction and a final X_{CO_2} greater than initial. If equilibrium was attained, the difference in P between that of the experiment and that for equilibrium between minerals and pure CO_2 fluid (thick shaded vertical bars) can be calculated from tabulated thermodynamic data just for mineral volumes and compressibilities and for the fugacity of CO_2 in CO_2-H_2O fluid solutions. Corrected values of P for carbonation and decarbonation experiments should be the same at each T within error of measurement. If equilibrium was not attained, corrected values of P for a pair of decarbonation and carbonation experiments at a given T will not be the same but will bracket the true P of equilibrium between minerals and pure CO_2.

Values of X_{CO_2} at the end of each experiment (Tables 1 and 2) were computed from measured CO_2 and H_2O losses from the inner capsule. The amount of CO present was estimated indirectly from the fraction of the H_2O loss attributable to H_2 diffusion and the stoichiometry of reaction 5. The fraction of the H_2O loss attributable to H_2 diffusion was taken as the total H_2O loss less H_2O adsorbed onto the measured amounts of silver oxalate and mineral reaction mix loaded into each inner capsule. The P corrections were computed from the data of Holland and Powell (1998, updated 2001). Corrections calculated from the data of Berman (1988, updated 1992) agreed with those computed from the data of Holland and Powell within ±100 bars, the resolution of calculations made with the THERMOCALC program of Holland and Powell. The P corrections are probably accurate because they only involve the molar volumes and compressibilities of minerals and the fugacity of CO_2 (f_{CO_2}) in CO_2-H_2O solutions.

If equilibrium was not attained in the experiments, the P correction underestimates the difference between P_{ex} and the P for equilibrium with pure CO_2 for experiments in which carbonation occurred and overestimates the difference for experiments in which decarbonation occurred. Thus, P_{cor} for carbonation and decarbonation experiments at a given T bracket the true P of equilibrium between minerals and pure CO_2 fluid regardless of the approach to equilibrium during the experiment.

RESULTS

Results of the phase-equilibrium experiments are summarized in Tables 1 and 2 and in Figures 2 and 3. Values of P_{cor} in experiments on reaction 3 differ by 100–200 bars between carbonation and decarbonation half-brackets at each T, indicating a high precision of the experiments. The equilibrium based on reaction 3 has been bracketed between 7.0 and 7.1 kbar at 800 °C, between 8.6 and 8.7 kbar at 850 °C, and between 10.5 and 10.7 kbar at 900 °C. The P correction for experiments at 800 °C resulted in an estimated P_{cor} 100 bars less for the carbonation half-bracket than for the decarbonation half-bracket (Table 1, Fig. 2). This apparent inconsistency, however, is within the precision of measurement of P_{ex} (±100 bars). Values of P_{cor} are within ±100 bars for four experiments at 850 °C and $P_{ex} = 8.9–9.3$ kbar with the amount of reaction varying between –50% (carbonation) and +100% (decarbonation), suggesting a close approach to mineral-fluid equilibrium and validating the procedure for correcting P.

Values of P_{cor} in experiments on reaction 4 differ by 200 bars between the narrowest carbonation and decarbonation half-brackets at 850 and 900 °C and by 600 bars at 800 °C, also indicating a high precision of the experiments. The equilibrium based on reaction 4 has been bracketed between 7.1 and 7.7 kbar at 800 °C, between 9.2 and 9.4 kbar at 850 °C, and between 10.7 and 10.9 kbar at 900 °C. Values of P_{cor} for four experiments at 850 °C and $P_{ex} = 8.8–10.2$ kbar correlate with % reaction, implying a somewhat greater departure from mineral-fluid equilibrium than in experiments involving Rt, Mgs, and Gk. The difference is consistent with the refractory char-

acter of Zrn.

Results are reported for experiments U18, U36, and U40 in Tables 1 and 2 and Figures 2 and 3, even though the Hem-Mag-H_2O buffer was not preserved in the outer capsule. If there had been significantly more reduction of CO_2 in these three experiments, the measured H_2O loss from the inner capsules should have been larger than in the others. The H_2O losses for experiments U18, U36, and U40, however, are within the range of H_2O losses for experiments that preserved the Hem-Mag-H_2O buffer (Tables 1 and 2). Experimental results for the three experiments therefore appear to be valid. Probably the outer capsule of experiments U18, U36, and U40 leaked slowly and retained Hem, Mag, and H_2O at least for the first 2 h when most of the H_2 diffused into the capsule from the sample assembly.

Discussion

Evaluation of thermodynamic properties of geikielite and zircon

The principal motivation of the experiments was to evaluate values for the thermodynamic properties of Gk and Zrn. Considering uncertainties in P (±300 bars) and T (±3 °C), curves for equilibria based on reactions 3 and 4, calculated from both the Berman (1988, updated 1992) and Holland and Powell (1998, updated 2001) databases, pass through all experimental brackets (Figs. 2 and 3). The experimental results therefore cannot identify any significant inaccuracies in the thermodynamic data for Gk or Zrn (or for Bd, Fo, Mgs, Rt, or CO_2).

The good agreement between calculated curves and experimental results in Figures 2 and 3, however, appears to be somewhat fortuitous. Typically, the principal source of uncertainty in thermodynamic calculations is the enthalpies of minerals that are mostly derived from laboratory phase-equilibrium experiments. Tabulated values of the enthalpy for Gk are derived from determinations of the equilibrium based on reaction 3 by Haselton et al. (1978) in reconnaissance experiments at 950–1250 °C and 13–26 kbar. A number of factors introduce relatively large uncertainties into any thermodynamic analysis of their results. The experiments were unreversed and attainment or bracketing of equilibrium was not assured. Fluid present during the experiments may not have been pure CO_2 because capsules were unsealed and hydrogen fugacity was not buffered. Uncertainties in P (±1 kbar) and T (±15 °C) were relatively large. Values of f_{CO_2} at the conditions of their experiments are not as well known as at lower P. Tabulated values of enthalpy for Zrn are derived from experiments by Schuiling et al. (1976) that bracketed the activity of SiO_2 defined by Zrn + Bd at 1000 K and 1 kbar between the value defined by sphene ($CaTiSiO_5$) + perovskite ($CaTiO_3$) and that defined by albite ($NaAlSi_3O_8$) + nepheline ($NaAlSiO_4$). The relatively large uncertainty in enthalpy derived for Zrn appears in Table 5 of Holland and Powell (1998) as a standard deviation for the enthalpy of Zrn that is larger on a percentage basis than for any other orthosilicate listed. Direct measurement of the enthalpy of Zrn by high-T solution calorimetry (Ellison and Navrotsky 1992) is also highly uncertain (±3.1 kJ/mol, standard error).

Experimental results of this study lead to more precise esti-

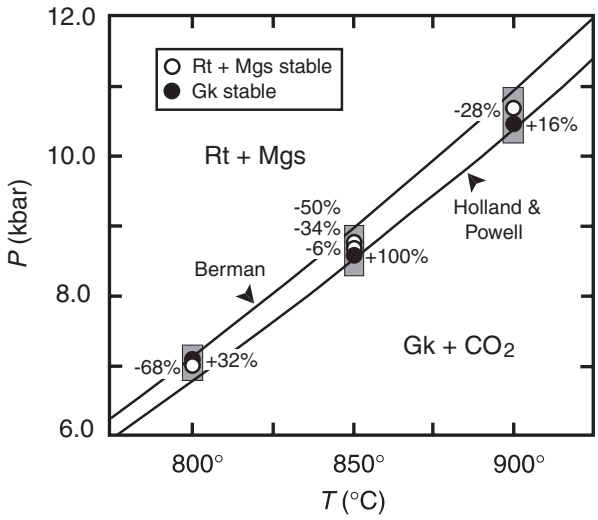

Figure 2. All experimental data from this study for reaction 3: Rt + Mgs = Gk + CO_2. Filled circles, conditions at which Gk is stable; open circles, Rt + Mgs stable. The P plotted for each experiment has been corrected to the value for equilibrium between minerals and a pure CO_2 fluid (see Fig. 1 and text). Numbers refer to % reaction (positive values denote decarbonation; negative values carbonation). Size of circles represents the precision of the control of P and T during the experiments (±100 bars, ±2 °C). Shaded rectangles represent the preferred experimental estimate of the location of the equilibrium considering the size of the narrowest bracket at each T and uncertainties in the accuracy in P (±300 bars) and T (±3 °C). Solid curves are the P-T conditions for the equilibrium computed from the thermodynamic databases of Berman (1988, updated 1992) and Holland and Powell (1998, updated 2001).

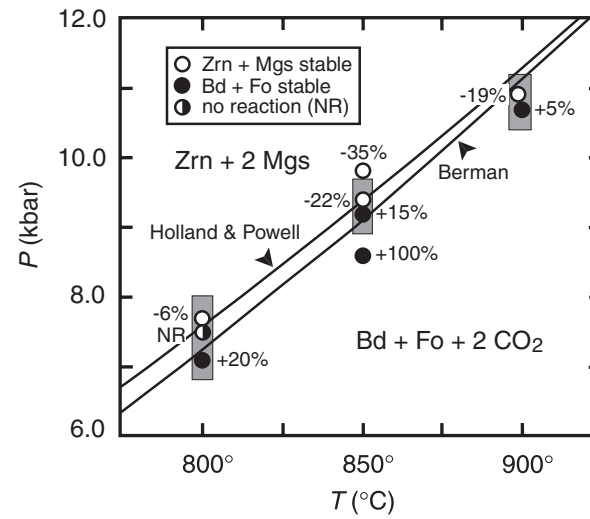

Figure 3. All experimental data from this study for reaction 4: Zrn + 2 Mgs = Bd + Fo + 2 CO_2. Filled circles, conditions at which Bd + Fo is stable; open circles, Zrn + Mgs stable; half-filled circle, no reaction. All other features the same as in Figure 2.

mates of the molar enthalpy of formation and molar Gibbs free energy of formation from the elements at 1 bar and 298 K ($\Delta_f\bar{H}^o$ and $\Delta_f\bar{G}^o$, respectively) for Gk and Zrn. Assuming that all thermodynamic data for Mgs, Rt, Fo, Bd, and CO_2 in Berman (1988, updated 1992) are correct and that data for the entropy, heat capacity, and molar volume of Gk and Zrn are correct, the most restrictive half-brackets in Tables 1 and 2 limit $\Delta_f\bar{H}^o$ and $\Delta_f\bar{G}^o$ for Gk and Zrn to the ranges listed in Table 3. A similar analysis leads to ranges in the values of $\Delta_f\bar{H}^o$ and $\Delta_f\bar{G}^o$ for Gk and Zrn consistent with the Holland and Powell (1998, updated 2001) database (Table 3). Estimates of $\Delta_f\bar{H}^o$ for Zrn, based on experimental data in Table 2 and the databases of either Berman or Holland and Powell (Table 3), are within error of measurement of the value determined using high-T solution calorimetry by Ellison and Navrotsky (1992), –2034.2 ± 3.1 (±1 standard error) kJ/mol. Results of this study confirm the accuracy of tabulated thermodynamic data for Gk and Zrn, and, more importantly, significantly reduce the uncertainty in those values. Calculations of phase equilibria involving Gk or Zrn using either the Holland and Powell or Berman databases therefore have been put on a firmer foundation.

Selected applications to field occurrences

Separation of geikielite and baddeleyite isograds. Isograds based on the prograde development of Gk and Bad by reactions 1 and 2 occur close together in contact aureoles. In the Ballachulish aureole, Scotland, for example, the Gk and Bd isograds occur at least 50 m but no more than 350 m apart (Ferry 1996a). The experimental data explain the small separation of the isograds. The brackets in Tables 1 and 2 require that the P-T curve for reaction 3 be no more than 40 °C higher and no more than 10 °C lower than the P-T curve for reaction 4 at 9 kbar, the midpoint of the range of pressures investigated. Reactions 1 and 2 are related to reactions 3 and 4 by:

$$\underset{\text{dolomite}}{CaMg(CO_3)_2} = \underset{\text{calcite}}{CaCO_3} + \underset{\text{magnesite}}{MgCO_3} \quad (6).$$

Because $\Delta\bar{G}^o$ of reaction 6 is small at the P-T conditions of the experiments [≈4–5 kJ, calculated from the data of Holland and Powell (1998, updated 2001)], Reactions 1 and 2 also must be close in P-T space. Calculated P-T curves for reactions 1 and 2 using the database of either Berman (1988, updated 1992) or Holland and Powell (1998, updated 2001) are <25 °C apart at any P within the range of the experiments, with the curve for reaction 1 at higher T than that for reaction 2. The close proximity of the Gk and Bad isograds in the field is a consequence of the close proximity of reactions 1 and 2 in P-T space at a given a_{CO_2}. The experimental data and thermodynamic calculations predict that the Bd isograd based on reaction 2 should lie at lower T and therefore farther from the intrusive contact in contact aureoles than the Gk isograd based on reaction 1. The opposite is observed in the Ballachulish aureole because mineral reactants and products of reaction 2 are pure substances or nearly so, whereas natural Gk in the Ballachulish aureole is an Mg-Fe solid solution with Mg/(Fe + Mg) = 0.48–0.59 near the Gk isograd. The reduced activity of $MgTiO_3$ in the Gk solid solution (estimated assuming ideal mixing) displaced the equilibrium based on reaction 1 to 20–60 °C below that of reaction 2 (the range in T displacement reflects the range in Gk compositions and differences between the thermodynamic databases used to make the estimate).

Fluid composition at the geikielite and baddeleyite isograds. The X_{CO_2} of fluid at the peak of metamorphism in Dol-Cal-Fo marbles bears on whether the carbonate rocks were infiltrated by reactive aqueous fluids (Ferry 1994). If X_{CO_2} is low, infiltration is indicated regardless of the geometry of fluid flow. If X_{CO_2} is high, either infiltration did not occur or the amount of fluid was small. Unfortunately the assemblage Dol-Cal-Fo typically contains no useful information about fluid composition. The development of Gk and Bd during prograde contact metamorphism in the Ballachulish aureole, Scotland, is an example of how calculation of X_{CO_2} from equilibria based on reactions 1 and 2, however, can provide estimates of fluid composition during metamorphism of Dol-Cal-Fo marbles. Pressure during contact metamorphism in the Ballachulish aureole was 3.0±0.5 kbar (Pattison 1991), and T at the peak of metamorphism at the Gk and Bd isograds was 640–650 °C and 660–710 °C, respectively [Ferry (1996a); uncertainty in T reflects uncertainty in the exact location of the isograds]. Values of X_{CO_2} were computed for each isograd using both the Berman (1988, updated 1992) and the Holland and Powell (1998, updated 2001) databases. Reduced activities of components in Cal, Dol, Fo, and Gk were estimated from analyses of minerals in outcrops that bracket the isograds in the field and from ideal ionic mixing models (Rt, Zrn, and Bd are pure substances). Specifically, X_{CO_2} at the Gk and Bd isograds was bracketed using mineral compositions in samples 7A and 7C and samples 7D and 8A, respectively, of Ferry (1996a, his Fig. 1). The measured compositions of Dol and Fo in sample 7D are $(Ca_{1.01}Mg_{0.95}Fe_{0.03}Mn_{0.01})(CO_3)_2$, and $(Mg_{1.91}Fe_{0.08}Mn_{0.01})SiO_4$, respectively. The compositions of Cal in samples 7D and 8A

TABLE 3. Constraints on enthalpy and Gibbs free energy of geikielite and zircon from reversed experiments*

	Consistent with Berman database†			Consistent with H-P database‡		
Function	Tabulated	Upper bound§	Lower bound#	Tabulated	Upper bound§	Lower bound#
$\Delta_f\bar{H}^o_{Gk}$	–1570.70	–1569.66	–1571.00	–1567.17	–1567.01	–1568.48
$\Delta_f\bar{G}^o_{Gk}$	–1482.31	–1481.27	–1482.61	–1478.72	–1478.56	–1480.03
$\Delta_f\bar{H}^o_{Zrn}$	–2031.90	–2030.80	–2033.30	–2031.82	–2031.49	–2034.46
$\Delta_f\bar{G}^o_{Zrn}$	–1917.39	–1916.29	–1918.79	–1917.31	–1916.98	–1919.95

* Enthalpy and Gibbs free energy of formation from the elements at 1 bar and 298 K in kJ/mol.
† Berman (1988, updated 1992).
‡ Holland and Powell (1998, updated 2001).
§ Upper bound is largest value consistent with the most restrictive experimental half-bracket.
# Lower bound is smallest value consistent with the most restrictive experimental half-bracket.

were those computed for equilibrium with Dol at 660 and 710 °C, respectively (Anovitz and Essene 1987). The composition of fictive Gk in sample 7A ($Mg_{0.73}Fe_{0.26}Mn_{0.01}TiO_3$) that would have formed had X_{CO_2} been less than the lower bound was estimated from the measured composition of Fo in the rock and the average of all measured values of $[(Mg/Fe)_{Fo}/(Mg/Fe)_{Gk}]$ and $[(Mg/Mn)_{Fo}/(Mg/Mn)_{Gk}]$ from the aureole. All other mineral compositions used in the calculations appear in Table 2 of Ferry (1996a). A range in X_{CO_2} values derives from differences in both T and mineral compositions for the samples that bracket each isograd. Using the Berman database, X_{CO_2} = 0.72–1.0 and 0.70–1.0 at the Gk and Bd isograds, respectively. Using the Holland and Powell database, X_{CO_2} = 0.54–0.88 and 0.74–1.0 at the Gk and Bd isograds, respectively. The high X_{CO_2} at the Gk and Bd isograds implies that little or no chemically reactive aqueous fluid infiltrated Dol-Cal-Fo marbles in the Ballachulish aureole at the peak of prograde metamorphism, consistent with earlier conclusions based on both stable isotopic (Hoernes et al. 1991) and petrologic (Ferry 1996b) studies.

Activity of CO_2 during UHP metamorphism. Estimates of X_{CO_2} during UHP metamorphism are <0.1 (Wang and Liou 1993; Zhang and Liou 1996). The low value of X_{CO_2} potentially is inconsistent with reported occurrences of Mgs + Rt and Mgs + Zrn rather than Gk or Bd + Fo in UHP rocks (e.g., Liou et al. 1995; Zhang and Liou 1996; Dobrzhinetskaya et al. 2001). The potential inconsistency was evaluated by computing the lower limit on a_{CO_2} required to stabilize Mgs + Rt instead of Gk and Mgs + Zrn instead of Bd + Fo during UHP metamorphism, i.e., a_{CO_2} recorded by equilibria based on reactions 3 and 4 at the low-P limit and over the range of T estimated for UHP metamorphism in general, T = 400–800 °C along the Qtz-Cs equilibrium (Liou et al. 1994). All minerals were considered pure substances. The calculated lower bound is the same regardless of the database used [Berman (1988, updated 1992) or Holland and Powell (1998, updated 2001)] or the equilibrium considered (based on reaction 3 or reaction 4), $2{\cdot}10^{-5}$ at 400 °C to $2{\cdot}10^{-2}$ at 800 °C. For metamorphism at P above the Qtz-Cs equilibrium, minimum values of a_{CO_2} would be lower still. The occurrence of Rt + Mgs and Zrn + Mgs in UHP metamorphic rocks therefore is fully consistent with low values of X_{CO_2} inferred independently from other mineral equilibria (Wang and Liou 1993; Zhang and Liou 1996). In spite of the not uncommon occurrence of carbonate minerals in UHP rocks, there is currently no evidence for CO_2-rich fluids during UHP metamorphism.

Activity of CO_2 during mantle metasomatism and kimberlite-genesis. Upper limits on a_{CO_2} in the mantle are recorded by the occurrence of Rt + Mg-rich ilmenite (Ilm) in rocks produced by mantle metasomatism (e.g., Zhao et al. 1999; Sobolev and Yefimova 2000) and by the occurrence of Zrn + Bd as megacrysts in kimberlites (e.g., Schärer et al. 1997). Specifically, the upper limits are defined by equilibria based on reactions 3 and 4 at the P-T conditions of equilibration of the mineral pairs. For example, application of reaction 3 to the occurrence of Ilm (X_{MgTiO_3} = 0.48) and Rt equilibrated with mica, orthopyroxene, and diopside at 36 kbar and 1027 °C in a sample of mantle-derived vein material (Zhao et al. 1999) limits a_{CO_2} to <0.18 during one instance of mantle metasomatism. The calculation considered Mgs to be a pure substance, assumed $a_{MgTiO_3} = X_{MgTiO_3}$ [appropriate for the composition of ilmenite at the conditions of equilibration (Ghiorso 1990)], and used the thermodynamic database of Holland and Powell (1998, updated 2001). Calculated a_{CO_2} is <0.17 if the database of Berman (1988, updated 1992) is used, and regardless of database, the upper bound decreases if a_{MgCO_3}<1. If results can be generalized, fluids causing mantle metasomatism evidently are not especially CO_2-rich. In principle, analogous constraints on a_{CO_2} may be placed on the conditions of kimberlite genesis from application of reaction 4 to occurrences of Bd + Zrn megacrysts, assuming coexistence with mantle olivine, provided that the P-T conditions of their equilibration may be estimated. Additional estimates of a_{CO_2} from equilibria based on reactions 3 and 4 and of oxygen fugacity from other equilibria involving Rt and Ilm (e.g., Zhao et al. 1999) will lead to a more complete chemical characterization of agents that effect melting and metasomatism in the mantle.

ACKNOWLEDGMENTS

Experiments were conducted while J.M.F. was a Visiting Professor at UCLA. He thanks Natalie Caciagli, Heather Lin, and Peter Tropper for advice in the piston-cylinder laboratory and Wayne Dollase for all X-ray diffraction measurements. We thank Andrea Koziol, Dave Pattison, and Bob Tracy for helpful reviews of the manuscript. Research supported by grant EAR-9805346 to J.M.F. and EAR-9909583 to C.E.M., both from the Division of Earth Sciences, National Science Foundation.

REFERENCES CITED

Anovitz, L.M. and Essene E.J. (1987) Phase equilibria in the system $CaCO_3$-$MgCO_3$-$FeCO_3$. Journal of Petrology, 28, 389–414.

Aranovich, L.Y. and Newton, R.C. (1998) Reversed determination of the reaction: Phlogopite + quartz = enstatite + potassium feldspar + H_2O in the ranges 750–875 °C and 2–12 kbar at low H_2O activity with concentrated KCl solutions. American Mineralogist, 83, 193–204.

Berman, R.G. (1988) Internally consistent thermodynamic data for minerals in the system Na_2O-K_2O-CaO-MgO-FeO-Fe_2O_3-Al_2O_3-SiO_2-TiO_2-H_2O-CO_2. Journal of Petrology, 29, 445–522.

Charlu, T.V., Newton, R.C., and Kleppa, O.J. (1975) Enthalpies of formation at 970 K of compounds in the system MgO-Al_2O_3-SiO_2 from high temperature solution calorimetry. Geochimica et Cosmochimica Acta, 39, 1487–1497.

Dobrzhinetskaya, L.F., Green, H.W. II, Mitchell, T.E., and Dickerson, R.M. (2001) Metamorphic diamonds: Mechanism of growth and inclusion of oxides. Geology, 29, 263–266.

Ellison, A.J.G. and Navrotsky, A. (1992) Enthalpy of formation of zircon. Journal of the American Ceramic Society, 75, 1430–1433.

Ferry, J.M. (1994) Role of fluid flow in the contact metamorphism of siliceous dolomitic limestones. American Mineralogist, 79, 719–736.

———(1996a) Three novel isograds in metamorphosed siliceous dolomites from the Ballachulish aureole, Scotland. American Mineralogist, 81, 485–494.

———(1996b) Prograde and retrograde fluid flow during contact metamorphism of siliceous carbonate rocks from the Ballachulish aureole, Scotland. Contributions to Mineralogy and Petrology, 124, 235–254.

Ghiorso, M.S. (1990) Thermodynamic properties of hematite-ilmenite-geikielite solid solutions. Contributions to Mineralogy and Petrology, 104, 645–667.

Haselton, H.T., Jr., Sharp, W.R., and Newton, R.C. (1978) CO_2 fugacity at high temperatures and pressures from experimental decarbonation reactions. Geophysical Research Letters, 5, 753–756.

Hoernes, S., MacLeod-Kinsel, S., Harmon, R.S., Pattison, D., and Strong, D.F. (1991) Stable isotope geochemistry on the intrusive complex and its metamorphic aureole. In G. Voll, J. Töpel, D.R.M. Pattison, and F. Seifert, Eds. Equilibrium and Kinetics in Contact Metamorphism. The Ballachulish Igneous Complex and its Aureole, p. 351–377. Springer-Verlag, New York.

Holland, T.J.B. and Powell, R. (1998) An internally consistent thermodynamic data set for phases of petrological interest. Journal of Metamorphic Geology, 16, 309–343.

Koziol, A.M. and Newton, R.C. (1995) Experimental determination of the reactions magnesite + quartz = enstatite + CO_2 and magnesite = periclase + CO_2, and enthalpies of formation of enstatite and magnesite. American Mineralogist, 80, 1252–1260.

———(1998) Experimental determination of the reaction: magnesite + enstatite = forsterite + CO_2 in the ranges 6–25 kbar and 700–1100 °C. American Mineralo-

gist, 83, 213–219.
Kretz, R. (1983) Symbols for rock-forming minerals. American Mineralogist, 68, 277–279.
Liou, J.G., Zhang, R., and Ernst, W.G. (1994) An introduction to ultrahigh-pressure metamorphism. The Island Arc, 3, 1–24.
———(1995) Occurrences of hydrous and carbonate phases in ultrahigh-pressure rocks from east-central China: Implications for the role of volatiles deep in cold subduction zones. The Island Arc, 4, 362–375.
Manning, C.E. and Boettcher, S.L. (1994) Rapid-quench hydrothermal experiments at mantle pressures and temperatures. American Mineralogist, 79, 1153–1158.
Newton, R.C. and Manning, C.E. (2000) Quartz solubility in H_2O-NaCl and H_2O-CO_2 solutions at deep crust-upper mantle pressures and temperatures: 2–15 kbar and 500–900 °C. Geochimica et Cosmochimica Acta, 64, 2993–3005.
Pattison, D.R.M. (1991) P-T-a(H_2O) conditions in the thermal aureole. In G. Voll, J. Töpel, D.R.M. Pattison, and F. Seifert, Eds. Equilibrium and Kinetics in Contact Metamorphism. The Ballachulish Igneous Complex and its Aureole, p. 327–350. Springer-Verlag, New York.
Rosenbaum, J.M. and Slagel, M.M. (1995) C-O-H speciation in piston-cylinder experiments. American Mineralogist, 80, 109–114.
Schärer, U., Corfu, F., and Demaiffe, D. (1997) U-Pb and Lu-Hf isotopes in baddeleyite and zircon megacrysts from the Mbuji-Mayi kimberlite: Constraints on the subcontinental mantle. Earth and Planetary Science Letters, 143, 1–16.
Schuiling, R.D., Vergouwen, L., and van der Rijst, H. (1976) Gibbs energies of formation of zircon ($ZrSiO_4$), thorite ($ThSiO_4$), and phenacite ($BeSiO_4$). American Mineralogist, 61, 166–168.
Sobolev, N.V. and Yefimova, E.S. (2000) Composition and petrogenesis of Ti-oxides associated with diamonds. International Geology Review, 42, 758–767.
Wang, X. and Liou, J.G. (1993) Ultra-high-pressure metamorphism of carbonate rocks in the Dabie Mountains, central China. Journal of Metamorphic Geology, 11, 575–588.
Zhang, R.Y. and Liou, J.G. (1996) Coesite inclusions in dolomite from eclogite in the southern Dabie Mountains, China: The significance of carbonate minerals in UHPM rocks. American Mineralogist, 81, 181–186.
Zhao, D., Essene, E.J., and Zhang, Y. (1999) An oxygen barometer for rutile-ilmenite assemblages: Oxidation state of metasomatic agents in the mantle. Earth and Planetary Science Letters, 166, 127–137.

MANUSCRIPT RECEIVED OCTOBER 30, 2001
MANUSCRIPT ACCEPTED JUNE 11, 2002
MANUSCRIPT HANDLED BY ROBERT J. TRACY